

The interweaving roles of mineral and microbiome in shaping the antibacterial activity of archaeological medicinal clays

Christidis, G. E.; Knapp, C. W.; Venieri, D.; Gounaki, I.; Elgy, C.; Valsami-Jones, E.; Photos-Jones, E.

DOI:
[10.1016/j.jep.2020.112894](https://doi.org/10.1016/j.jep.2020.112894)

License:
Creative Commons: Attribution-NonCommercial-NoDerivs (CC BY-NC-ND)

Document Version
Peer reviewed version

Citation for published version (Harvard):
Christidis, GE, Knapp, CW, Venieri, D, Gounaki, I, Elgy, C, Valsami-Jones, E & Photos-Jones, E 2020, 'The interweaving roles of mineral and microbiome in shaping the antibacterial activity of archaeological medicinal clays', *Journal of Ethnopharmacology*, vol. 260, 112894. <https://doi.org/10.1016/j.jep.2020.112894>

[Link to publication on Research at Birmingham portal](#)

General rights

Unless a licence is specified above, all rights (including copyright and moral rights) in this document are retained by the authors and/or the copyright holders. The express permission of the copyright holder must be obtained for any use of this material other than for purposes permitted by law.

- Users may freely distribute the URL that is used to identify this publication.
- Users may download and/or print one copy of the publication from the University of Birmingham research portal for the purpose of private study or non-commercial research.
- User may use extracts from the document in line with the concept of 'fair dealing' under the Copyright, Designs and Patents Act 1988 (?)
- Users may not further distribute the material nor use it for the purposes of commercial gain.

Where a licence is displayed above, please note the terms and conditions of the licence govern your use of this document.

When citing, please reference the published version.

Take down policy

While the University of Birmingham exercises care and attention in making items available there are rare occasions when an item has been uploaded in error or has been deemed to be commercially or otherwise sensitive.

If you believe that this is the case for this document, please contact UBIRA@lists.bham.ac.uk providing details and we will remove access to the work immediately and investigate.

Journal Pre-proof

The interweaving roles of mineral and microbiome in shaping the antibacterial activity of archaeological medicinal clays

G.E. Christidis, C.W. Knapp, D. Venieri, I. Gounaki, C. Elgy, E. Valsami-Jones, E. Photos-Jones

PII: S0378-8741(19)33462-2

DOI: <https://doi.org/10.1016/j.jep.2020.112894>

Reference: JEP 112894

To appear in: *Journal of Ethnopharmacology*

Received Date: 8 September 2019

Revised Date: 27 March 2020

Accepted Date: 16 April 2020

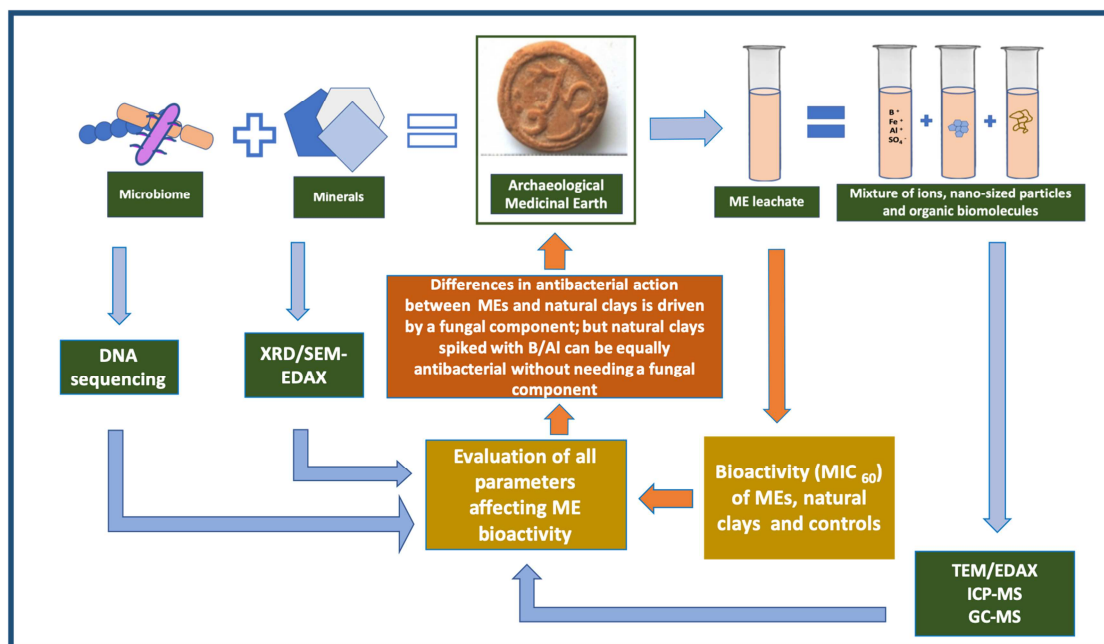
Please cite this article as: Christidis, G.E., Knapp, C.W., Venieri, D., Gounaki, I., Elgy, C., Valsami-Jones, E., Photos-Jones, E., The interweaving roles of mineral and microbiome in shaping the antibacterial activity of archaeological medicinal clays, *Journal of Ethnopharmacology* (2020), doi: <https://doi.org/10.1016/j.jep.2020.112894>.

This is a PDF file of an article that has undergone enhancements after acceptance, such as the addition of a cover page and metadata, and formatting for readability, but it is not yet the definitive version of record. This version will undergo additional copyediting, typesetting and review before it is published in its final form, but we are providing this version to give early visibility of the article. Please note that, during the production process, errors may be discovered which could affect the content, and all legal disclaimers that apply to the journal pertain.

© 2020 Published by Elsevier B.V.



Graphical abstract



The interweaving roles of mineral and microbiome in shaping the antibacterial activity of archaeological medicinal clays

G.E. Christidis¹, C.W. Knapp², D. Venieri³, I. Gounaki³, C. Elgy⁴,
E. Valsami-Jones⁴, E. Photos-Jones^{5,6*}

*effie.photos-jones@glasgow.ac.uk

1. School of Mineral Resources Engineering, Technical University of Crete, 73100 Chania, Greece

2. Civil and Environmental Engineering, University of Strathclyde, Glasgow G1 1XQ, UK

3. School of Environmental Engineering Technical University of Crete, 73100 Chania, Greece

4. School of Geography, Earth and Environmental Sciences, University of Birmingham, Edgbaston, Birmingham B15 2TT, UK

5. Analytical Services for Art and Archaeology (Ltd), Glasgow G12 8JD, UK

6. Archaeology, School of Humanities, University of Glasgow, Glasgow G12 8QQ, UK

Abstract

Ethnopharmacological relevance: Medicinal Earths (MEs), natural aluminosilicate-based substances (largely kaolinite and montmorillonite), have been part of the European *pharmacopoeia* for well over two millennia; they were used generically as ‘antidotes to poison’

Aim of the study: To test the antibacterial activity of three Lemnian and three Silesian Earths, medicinal earths in the collection of the Pharmacy Museum of the University of Basel, dating to 16th-18th century and following a prescribed methodology (see graphical abstract). To assess and prioritize the parameters which drive their antibacterial activity, if present.

Materials and Methods: The medicinal earths are characterised chemically (ICP-MS), mineralogically (both bulk (XRD) and at the nano-sized level (TEM-EDAX)); their organic load (bacterial and fungal) is DNA-sequenced; their bioactivity (MIC₆₀) is tested against Gram-positive, *S. aureus* and Gram-negative, *P. aeruginosa*. The bioactivities (MIC₆₀) of natural clays from Lemnos, N Aegean, and Melos, SW Aegean, spiked with Al, Fe, Ti, and B are also tested against the same pathogens for purposes of comparison.

Results. Not all MEs are antibacterial. Of the three Lemnian Earths, only two are antibacterial against both pathogens; of the Silesian Earths only one is mildly antibacterial and against Gram-negative pathogen, only. The bioactivity of the two Lemnian Earths is driven by a fungal component, *Talaromyces spp*, a fungus of the family of *Trichocomaceae* (order Eurotiales), historically associated with *Penicillium*. This fungus was not found in the natural Lemnos clays examined here. Comparable bioactivity with that of the two Lemnian Earths can be obtained from kaolinitic/smectitic clays spiked with B or Al.

Conclusions. It is not known whether archaeological medicinal earths were used as antibacterials, over and above as absorbants of toxins. Nevertheless, some display antibacterial properties which appear to have their origins in an organic (fungal) load.

Keywords: medicinal earths, Lemnian, Silesian, bioactivity, *Talaromyces spp*, mineral, nanoparticle, antimicrobial resistance

1.Introduction

Medicinal Earths (MEs) have been part of the European *pharmacopoeia* for well over two millennia. Stamped medicinal earths or *terra sigillata* are natural aluminosilicate-based substances (largely kaolinite and montmorillonite) with a well-recorded history of use as ‘antidotes to poison’ and spanning over two and a half millennia (Macgregor, 2013). Stamping the earth with a readily identifiable seal conferred confidence on the product but also provided control of the trade in such substances from antiquity to modern times (Nutton 2004). Lemnian Earth (LE), from the island of Lemnos, N.E. Aegean, was the oldest and most established and with continuous use until the early 20th century (Hasluck, 1910; Sealy, 1919). It is reported, amongst others, in Theophrastus (4th c BC), Dioscorides (1st c AD) and Pliny (2nd c AD). Galen (2nd c AD) visited the island and gave a detailed account of the various stages in the process of extraction and ‘washing’ thereof, both activities purported to have taken place once a year (Brock 1929, 185). Sometime in Late Antiquity and early Byzantine times the practice appears to have waned or stopped completely but it was certainly revived in the Ottoman period when its extraction and distribution was tightly regulated (Hasluck and Hasluck, 1929; Tourptsoglou-Stephanidou, 1986). As a result, many new MEs began to appear in the markets across the Mediterranean, Northern Europe and the Middle East aiming to emulate (and rival) LE’s widely acknowledged beneficial properties. Most carried the same tradition of being stamped, hence their generic name, *terra sigillata*.

In the 16th c the most prominent medicinal earth emerging out of Central Europe was Terra Silesia, in present day SW Poland (Dannenfeldt, 1984). It was also a *terra sigillata* since it bore the coat of arms of the city of Striga (Strigovia, Striegau, or Strzegom) consisting of three mountain peaks (see Fig. 1f). Terra Silesia acquired quite a reputation with doctors following the Paracelsus school who attributed its healing properties to the gold within the local auriferous granite. Medicinal earths from varying localities survive to this day in a number of museum collections as collectors’ curiosities (Duffin, 2013). Only very few have been subjected to analysis (Hardy and Rollinson 2016).

Over many years we have carried out research into some of the minerals discussed in the Greco-Roman technical and medical texts, from the perspective of geo-archaeological work and in an attempt to locate them in the field (Photos-Jones and Hall, 2011; Photos-Jones et al., 2015, 2016). We have suggested reasons why LE would have been efficacious, based on sampling of local sedimentary clays from the purported area of its extraction (Kotsinas, N.E. Lemnos) (Hall and Photos-Jones, 2008). Recently we have analysed three samples of Lemnos *terra sigillata* (we will refer to them as Lemnian Earth) in the collection of the Pharmacy Museum of the University of Basel (Fig. 1a-c) and qualitatively assessed their antibacterial activity (Photos-Jones et al., 2017).

This paper revisits the same three samples of Lemnian Earth (Fig. 1a-c: 700.4, 700.17, 700.18) in an attempt to assess the same activity, quantitatively, (MIC₆₀), against two pathogens (Gram-negative *P. aeruginosa* and Gram-positive *S. aureus*). These specific bacterial strains were chosen because of their relation to public health issues, and their use as valuable bacterial indicators. Further, it compares their efficacies as antibacterials with a contemporary set of Silesian Earths (Fig. 1d-f 703.1, 703.2, 703.3), also dating to 16th-18th century AD. Although all six MEs were purported to

be medicinal, only two were found to be demonstrably antibacterial, and against both of the above pathogens. Suffice it to say that clays can still be considered ‘medicinal’ even though they might display no antibacterial action. Antibacterial action is a property that we are interested in because it is easily measurable and quantifiable. We therefore asked the question: which parameters drive differences in antibacterial action between different samples of medicinal earths? Is it their mineralogy, at both bulk and nanosized level? or is it their elemental composition? or other factors?

By other factors we refer to the MEs’, natural or acquired organic load, their bacterial and fungal microbiome. Bacteria and fungi, naturally present within soils, can potentially have the inadvertent effect of rendering the clays medicinal (as antioxidants, antibacterials or metal chelators) on account of their production of secondary metabolites (e.g., Keller, 2019; Pettit, 2011). This is the result of either intra- and inter-specific interactions (Tyc et al., 2016), or toxicological conditions, the presence of metals (Locatelli et al., 2016) or salts (Medina et al., 2015). It can also be the result of their growth conditions. Ecologically, the production of secondary metabolites is advantageous to the microorganism since it increases its competitiveness or survival in the environment (Macheleidt et al., 2016).

We therefore propose a step-by-step investigation of the MEs, from the perspective of bulk mineralogy, chemistry of the leachate, and nanoparticle characterization, followed by DNA sequencing of their microbiome, and MIC₆₀ testing, against specific pathogens in order to shed light into the contribution of individual components to the MEs’ bioactivity. The graphical abstract at the start of the paper illustrates our proposed method which consists of the undertaking of a number of analytical techniques aimed to evaluate: a. the bulk mineral (XRD); b. the mineral leachate (TEM/EDAX/ICP-MS); c. the organic constituent (DNA sequencing of biome/GC-MS of secondary metabolites); d. the testing of bioactivity against select pathogens. In this study we have not undertaken the investigation of secondary metabolites (via GC-MS) but refer to them in previous work (Photos-Jones et al., 2017).

Having outlined our approach, (graphical abstract), we shall demonstrate that some clay samples can be rendered antibacterial on account of specific elements and/or nanosized particles, while others, with similar mineralogy, can be rendered antibacterial on account of their microbiome, bacterial or other. Demonstrating the idea that there might be multiple drivers to antibacterial activity within the same type of clay could potentially have far reaching implications.

Resistance against effective antibiotics has emerged as a serious and growing phenomenon in contemporary medicine, making the growth inhibition of virulent pathogens for humans and the environment quite a challenge (Manaia et al., 2016; Venieri et al., 2017a, 2017b). Clays have the potential to exhibit bactericidal effect in both Gram-negative and Gram-positive strains through the exchange of components between them and bacteria and the ultimate prevention of the latter’s metabolic functions (Haydel et al., 2008). Clay nanoparticles- based techniques have already been introduced to induce antibacterial action within aquatic environments and during water treatment (Unuabonah and Taubert, 2014). Although bacteria are considered very adaptive to hostile conditions, up until now no resistance mechanism similar to that against antibiotics has been recorded in clays (i.e. induction of antibiotic resistance genes).

Archaeological medicinal earths are clay-based and have an uninterrupted history of use (in the case of LE) of over two millennia. It is not clear whether they were intended as antibacterials, and not merely as absorbants of toxins. Nevertheless, with this paper and the one preceding it (Photos-Jones et al., 2017) we have demonstrated that some *can* be antibacterial. What we seek to understand is the parameters driving this antibacterial behaviour in a small number of archaeological medicinal clays.

INSERT FIG. 1



Fig. 1a 700.4
Lemnian Earth
Mus. No 01432

Fig. 1b 700.17
Lemnian Earth
Mus. No 01422

Fig. 1c 700.18
Lemnian Earth
Mus. No 01424

Fig. 1d 703.1
Terra Silesia
Mus. No 01114

Fig. 1e 703.2
Terra Silesia
Mus. No 01133

Fig. 1f 703.3
Terra Silesia.
Mus. No 01137

2. Materials and Methods

2.1 Materials

A total of eighteen samples were examined in this study; they fall into three groups:
a. six MEs consisting of three from Lemnos (LEs) (700.4, 700.17 and 700.18) and three from Silesia (SEs) (703.1, 703.2, 703.3). This group of samples derive, as mentioned earlier, from the collection of the Museum of Pharmacy, University of Basel (museum accession numbers are given in Fig. 1).

b. four natural clays consisting of two from Lemnos, N.E. Aegean (700.19 and 700.20) from the area of Kotsinas, NE Lemnos, the purported area of extraction of LE and another two from Melos, S.W. Cyclades. The Melos bentonite sample (933) originates from the Angeria mine, N.W. Melos, and the Melos kaolin sample (900.9) from the abandoned kaolin mine at Loulos, 2 km north of the Paleochori Bay, S.E. Melos. The Melos samples are introduced here as ‘good’ basic clays with which to build synthetics. c. eight synthetic samples prepared from Melos bentonite and kaolin and spiked with four different elements (i.e. Ti, Al, Fe, and B). These include Melos smectite and kaolinite treated with aluminum sulfate ($\text{Al}_2(\text{SO}_4)_3 \cdot 16\text{H}_2\text{O}$), (samples 6 and 7 respectively); smectite and kaolinite treated with boric acid (H_3BO_3) (samples 4 and 5, respectively); smectite and kaolinite treated with natural fine iron oxides collected from the island of Kea, N Cyclades, (Photos-Jones et al., 2018)(samples 14 and 15, respectively); and finally, smectite and kaolinite treated with analytical grade TiO_2 (anatase, Merck) (samples 10 and 9 respectively). The Kea samples have been chosen on account of the purity/finesse of their iron oxides and their recorded use from the 4th c BC.

The synthetic aluminium sulfate- and boron- treated samples were prepared as follows. 1g of clay (kaolin or bentonite) were placed in 50ml polyethylene centrifuge tubes. 15 ml of 1N H_3BO_3 or 0.5 N $\text{Al}_2(\text{SO}_4)_3$ (both of Sigma Aldrich analytical grade) solution were added, the clays were dispersed in an ultrasonic probe for 20s, and the tubes were covered with a stopper and left overnight. Subsequently, the suspensions were centrifuged, the clear supernatant solutions were decanted and the

whole procedure was repeated. In the following day the suspensions were centrifuged and the tubes with the clay were dried at 60°C and the dry clay powders were transferred in glass vials and stored. The synthetic samples with addition of iron oxides and TiO₂ were prepared by adding 0.1 g to 0.4 g of bentonite or kaolin. The materials were ground with an agate pestle and mortar using acetone to obtain fine grained homogeneous mixtures.

2.2 Methods

2.2.1 Mineralogy - XRD

The mineralogical composition of all samples was determined with X-ray diffraction (XRD), at the School of Mineral Resources Engineering, Technical University of Crete, on a Bruker D8 Advance Diffractometer equipped with a Lynx Eye strip silicon detector, using Ni-filtered CuK α radiation (35 kV, 35mA). Data were collected in the 2 θ range 3-70° 2 θ with a step size of 0.02° and counting time 1 s per strip step (total time 63.6 s per step). The XRD traces were analyzed and interpreted with the Diffrac Plus software package from Bruker and the Powder Diffraction Files (PDF). The quantitative analysis was performed on random powder samples (side loading mounting) by the Rietveld method using the BMGN code (Autoquan© software package version 2.8).

2.2.2 Bioactivity testing

2.2.2.1 Bacterial strains and antimicrobial tests

The bacterial indicators used for the assessment of antimicrobial properties of the samples were *Pseudomonas aeruginosa* NCTC 10662 (Gram-negative) and *Staphylococcus aureus* NCTC 12493 (Gram-positive). Both bacteria were cultured on LB agar (LABM) and LB broth (LABM) and the desired bacterial concentration in each experimental run was adjusted based on the McFarland scale, according to which, an inoculum absorbance of 0.132 measured at 600 nm corresponds approximately to a cell density of 1.5×10^8 CFU/mL. Our goal in this study was to employ both a Gram-negative and a Gram-positive species, considering their structural differences and physiology, which impose adverse behaviour in stressed environmental conditions. Both bacteria are often reported for their notable antibiotic resistance and their adaptability in hostile surroundings (Swetha et al. 2010; Venieri et al. 2017b).

2.2.2.2 Sample preparation and antimicrobial tests

The antibacterial activity of the samples was assessed over both bacterial indicators using their aqueous leachates. All leachates were prepared at a concentration of 600 mg/mL, mixing samples with sterile deionized water, followed by ultrasonication (Julabo ultrasonic bath) for 30 min at 25 °C and centrifugation at 10000 g for 15 min to remove all solids from the solution. The leachate was decanted, sterilized in the autoclave (20 min, 120 °C), and tested against bacteria.

In order to compare the difference in activity of samples with and without organic content, chemical oxidation was performed to breakdown organic matter with sodium hypochlorite (NaOCl) as the oxidizing agent (Anderson, 1963). An aliquot 4 mL of a NaOCl (6%) solution was mixed with of 2g of each sample into a centrifuge tube, which was then placed in a boiling water bath for 15 min. Then, the sample was centrifuged at 800 g for 10 min and the solution was decanted. The procedure was repeated 3 times, after which the solid was washed with sterilized water, dried and

processed for further biological analysis. For reference to this protocol, see Andrews (2001).

Antimicrobial activity of all samples (prior to and post chemical oxidation) was studied using the broth microdilution method and estimating the Minimum Inhibitory Concentration that inactivated 60% of the bacterial population (MIC_{60}). MICs were measured labeling 96-well sterile microtiter trays with dilutions of each sample. The bacterial inoculum in each case was adjusted to 10^5 CFU/mL. Microtiter trays were incubated at 37°C for 18-24 h, followed by optical density measurement at 630 nm, using a microplate reader (Labtech LT-4000 Plate Reader) and Manta LML software.

2.2.3 Chemical analyses of leachates-ICP-MS

The aqueous leachates were produced by adding 0.2 g of the samples in 5 ml distilled water, dispersing with ultrasonic probe for 20 s, allowing standing for 1 h and subsequent centrifugation. The supernatant was stored in polyethylene bottles for ICP-MS analysis (7500CX coupled with Autosampler Series 3000, both by Agilent Technologies) for major and trace elements. The precision of the analyses was tested using elemental standards (1000mg/L) by Merck. The relative standard deviation of the analyses varied according to the concentration, typically 7% for the major elements, less for the trace elements.

2.2.4 TEM-EDAX

For Transmission Electron Microscopy (TEM) with EDAX approximately 10mg of powder were suspended in 10ml of ultrapure water. The suspension was vortexed for 1 minute at full power (Rotamixer Hook and Tucker Ltd.) The sample was processed in the ultrasonic bath for 5 minutes (Branson 1510 ultrasonic bath) and centrifuged in 15ml tubes in the Eppendorf centrifuge 5804R, at 4,000rpm for 10 minutes for clay samples, and at 2,500rpm for 11 minutes for iron oxide samples, to remove particles above 450nm. A drop of 35 microliters of the supernatant was deposited onto 200mesh copper grids with carbon film and left there without drying for one hour. The excess sample was wicked from the grid, and the grid was washed 4x in water to remove any salts. The grid was dried for 16 hours before use. TEM images and EDX measurements were performed by the Birmingham University Centre for Electron Microscopy, using a Jeol 2100 microscope.

2.2.5 Particle size analysis

Particle size for the samples were measured by DLS using a Malvern Instruments Zetasizer nano ZS with a red (366 nm) laser. A method was developed to remove the larger particles and provide stable suspensions of the smaller particles for DLS analysis. The powders were dispersed in a 0.2% suspension of Novachem surfactant (Postnova Analytics UK Ltd.) in ultrapure water. The suspension was shaken thoroughly, vortexed (Rotamixer, Hook and Tucker Ltd.) at full power for 30 s and treated in the ultrasonic bath (Branson, 1510) for 5 min. The samples were centrifuged at 3000 rpm, for 5 min in 15 ml tubes using an Eppendorf 5804R centrifuge. This removed the larger particles from the samples. Stable suspensions were obtained under these conditions.

The zeta potential measurements of these suspensions were negative, and between –40 and –50 mV, due to the effect of the Novachem surfactant which produced a high surface charge. It follows that the zeta potential was altered and so is not representative of the original material. However, this enabled us to stabilise the suspensions and allowed reproducible size measurements to be made for the smallest particulate size fraction.

2.2.6 DNA sequencing

DNA were extracted using MoBio PowerSoil Extraction kits (Qiagen) according to manufacturer's procedures, except sample materials were agitated using a FastPrep24 cell homogenizer (MP Biomedicals; 6.0 speed, 2 x 20 seconds). Additionally, samples were initially incubated at 70°C for 10 minutes to facilitate the DNA extraction from Gram-positive microorganisms.

Purity and quantity of extracted DNA were measured using UV-microspectrophotometry. Extracts are stored at -80°C and further handled under UV-irradiated biological cabinets with HEPA-filter laminar-flow air flow. Samples were routinely diluted 1:50 with molecular-grade water to minimize inhibitors and improve reaction efficiency of downstream processes.

Polymerase chain reaction (PCR) was used to selectively target the hypervariable V4 region of the 16S-rRNA gene. Primers were forward (AYTGGGYDTAAAGNG; position 563-577) and combined set of reverse (TACNVGGGTATCTAATCC, TACCRGGGTHCTAATCC, TACCAGAGTATCTAATTC, and CTACDSRGGTMTCTAATC; position 907-924). To minimize cost, primers were further 'bar-coded' with a short 8-base genetic sequence to allow multiple samples to be simultaneously sequenced and sorted post-analytically using RDP initial pipeline bioinformatics tool (Cole et al., 2014; <http://pyro.cme.msu.edu/> <<https://mail.campus.gla.ac.uk/owa/redir.aspx?C=QAAlSmAq6PZR-ZWaTX0sUwu9AOPrSgI-UF8DmdH3dbzOhsDWft3UCA..&URL=http%3a%2f%2fpyro.cme.msu.edu%2f>>).

The presence of fungal and chloroplast DNA were tested by PCR with primers targeting the 18S-rRNA gene (Hadziavdic et al., 2014) and 16S-rRNA gene of chloroplasts, using aforementioned bacterial forward primer (position 563-577) and the CYAN-786-a probe modified to become a reverse primer (Knapp and Graham, 2004), respectively.

Subsequent analysis found previous universal primers for detecting fungus failed to detect members *Talaromyces* spp. As such, additional de novo primers were designed (in this study) for the detection of *Talaromyces* sp. (via intergenic spacer region) based on Genbank accession (JN899375) using NCBI's Primer-BLAST online design tool: TTGAGGGCAGAAATGACGCT (forward, 5'-3') and TGAAGAACGCAGCGAAATGC (reverse, 5'-3'). In silico analysis of primer specificity via BLASTn predict detection of *Talaromyces* spp. and *Penicillium* spp., both of the Trichocomaceae family of Eurotiales order.

Each 100µL PCR reaction mixture consisted of 10µL of diluted DNA sample, 50µL Taq PCR Master Mix kit (Qiagen; consisting of 1.5 mM MgCl₂, 2.5 units of Taq DNA polymerase, 1x proprietary PCR buffer, and 200 mM of each dNTP), 10µL 10x-

primer mixture (0.2 μ M final concentration of each primer). Reaction conditions were as follows, on a BioRad iCycler5 (BioRad, Hercules, CA USA) instrument: 3-min initial denaturation (94°C); 30 cycles of: denaturation (30s at 94°C), primer annealing (30s at temperatures specific for each assay: 58°C for 16S-rRNA and chloroplast, and 60°C for *Talaromyces*), and product extension (1 min at 72°C); and a final extension (10 min at 72°C). When completed, the instrument maintained the samples at 8°C.

To remove excess primers and un-polymerised nucleotides for bacterial DNA sequencing, PCR product were purified using QiaQuick PCR Purification kit (Qiagen). Quantities of PCR product were quantified by UV micro-spectrophotometrically, combined, and condensed to 30mL, > 20 ng/mL. Library preparation (e.g., adapter ligation) and MiSeq high-throughput sequencing (Illumina) were conducted by GATC-Biotech (Konstanz, Germany) with full quality-control and quality-assurance. The number of MiSeq reads per sample varied. Phylogenetic identity of each sequence was determined based on alignments with the “Classifier” function (Wang et al., 2007) of the RDPpipeline, which maintains databases for 16S- (and 18S-) rRNA sequences (Cole et al., 2014). The bootstrap cut-off was predetermined to be 70% based on sequence length.

3. Results

3.1 The mineralogy of MEs and natural clays

Table 1 shows the results of XRD analysis of six MEs and the four natural clays from Melos and Lemnos. LE 700.4 and 700.17 consist of kaolinite, illite and quartz, with dolomite being the dominant phase in 700.4 and hematite being a minor phase in 700.17. 700.18 consists of smectite, quartz, illite and albite. The Silesian Earths (SEs) are primarily kaolinite with illite with varying amounts of quartz and small quantities of anatase. Melos 900.9 and 933 are natural kaolinitic and smectitic clays respectively, while chlorite and alunite are present in natural Lemnos clays (700.19 and 700.20). Varying amounts of iron oxide are present in the three red samples (703.2, 700.17, 700.19).

INSERT TABLE 1

Table 1 XRD analyses of Silesian and Lemnian Earths; also, geological samples from Kotsinas, Lemnos, 700.19 and 700.20 and geological samples from Melos 933 and 900.9 (see discussion) included here for purposes of comparison; n.d. = not detected. Samples with asterisk (700.4, 700.17, 700.18, 700.19 and 700.20) were first published by Photos-Jones et al (2017).

Mineralogical Composition	703.1 Terra Silesia	703.2 Terra Silesia	703.3 Terra Silesia	700.4* Terra Lemnia	700.17* Terra Lemnia (after Photos-Jones et al 2017)*	700.18* Terra Lemnia	700.19* Natural red clay from Kotsinas, Lemnos	700.20* Natural clay from Kotsinas, Lemnos	933 natural smectite (Melos)	900.9 natural Kaolin (Melos)
Dolomite	n.d.	n.d.	n.d.	65.2	n.d.	n.d.	n.d.	n.d.	n.d.	n.d.
Kaolinite	31.2	87.9	67.4	17.3	37.4	n.d.	69.3	1	6.3	48.6
Smectite/montmorillonite	n.d.	n.d.	n.d.	n.d.	n.d.	66	n.d.	35.1	71.7	n.d.
Quartz	32.8	n.d.	25.8	7.6	17.7	6.9	n.d.	21	0.2	28.9

Opal-CT/ cristoballite	n.d.	n.d.	n.d.	n.d.	n.d.	n.d.	4.5	n.d.	n.d.	5.9
Illite	28.1	n.d.	6.5	9.9	41	18.1	n.d.	13.3	n.d.	n.d.
Anatase	1.2	4.6	0.3	n.d.	n.d.	n.d.	n.d.	n.d.	1.3	0.1
Albite	n.d.	n.d.	n.d.	n.d.	n.d.	9	n.d.	12.7	n.d.	n.d.
Alunite	n.d.	n.d.	n.d.	n.d.	n.d.	n.d.	22.5	n.d.	n.d.	3.3
Biotite	n.d.	n.d.	n.d.	n.d.	n.d.	n.d.	n.d.	n.d.	n.d.	n.d.
Calcite	n.d.	n.d.	n.d.	n.d.	n.d.	n.d.	n.d.	8.1	5.2	n.d.
Chlorite	n.d.	n.d.	n.d.	n.d.	n.d.	n.d.	n.d.	8.9	n.d.	n.d.
Halite	n.d.	n.d.	n.d.	n.d.	n.d.	n.d.	n.d.	n.d.	n.d.	6.2
Hematite	n.d.	7.5	n.d.	n.d.	3.8	n.d.	1.8	n.d.	n.d.	n.d.
K-Feldspar	6.7	n.d.	n.d.	n.d.	n.d.	n.d.	n.d.	n.d.	14.8	n.d.
Natroalunite	n.d.	n.d.	n.d.	n.d.	n.d.	n.d.	n.d.	n.d.	n.d.	7
Pyrite	n.d.	n.d.	n.d.	n.d.	n.d.	n.d.	n.d.	n.d.	0.5	n.d.
Tridymite	n.d.	n.d.	n.d.	n.d.	n.d.	n.d.	1.9	n.d.	n.d.	n.d.

402

403 In summary, the six archaeological and the four natural clay samples are broadly
 404 classified as either kaolinitic (700.17, all SEs, 700.19 and 900.9) or as smectitic
 405 (700.18, 700.20 and 933). 700.4 is primarily dolomitic with some kaolinite. In the
 406 section that follows we proceed to establish which of the above are bioactive.

407

408 3.2. Antibacterial activity of MEs, natural and synthetic clays

409

410 We first investigate the antibacterial activity of the six archaeological samples and the
 411 two Lemnos natural clays (700.19, 700.20) (Fig. 2 and Suppl file 1). The MIC₆₀ of the
 412 LEs is significantly lower than the MIC₆₀ of the SEs. The ranges of MIC₆₀ values of
 413 LE were 50-90 mg/mL and 12.5-45 mg/mL for *P. aeruginosa* and *S. aureus*,
 414 respectively, with the leachate of 700.17 being more active than the others. The
 415 respective MIC₆₀ values for SE were 66-264 mg/mL for *P. aeruginosa* and 132
 416 mg/mL for *S. aureus*, respectively. The order of bioactivity of the original samples
 417 towards the Gram-negative *P. aeruginosa* is 700.17 and 700.18 > 703.1 > 700.4 >
 418 703.2 > 703.3; The order of bioactivity of samples towards the Gram-positive *S.*
 419 *aureus* is 700.17 > 700.18 > 700.4 > all 703 series samples. However, the aqueous
 420 leachates of 703.1; 703.2 and 703.3 can hardly be described as “antimicrobial”,
 421 because the obtained MIC₆₀ values were considerably over 50 natural mg/mL. Natural
 422 clay samples 700.19 and 700.20 show low to no bioactivity. A sample of natural near
 423 pure alunogen (Al₂(SO₄)₃·17H₂O) from the solfatara at Fyriplaka, SE Melos (sample
 424 3), displayed here for purposes of comparison, is the most bioactive.

425

426 In summary, only two LEs (700.17, 700.18) are bioactive; 700.4, a dolomitic clay
 427 with small amounts of kaolinite, is not bioactive against *P. aeruginosa*. Lemnos
 428 natural clays 700.19, 700.20 and all the SEs (703.1, 703.2 and 703.3) are not bioactive
 429 following the criteria implemented here (MIC₆₀ < 50mg/ml). Given that kaolinite-
 430 rich clays can be *both* bioactive (700.17) *and* non-bioactive (700.19, 703.2) we
 431 suggest that mineralogy is not a key factor driving bioactivity. The same conclusion
 432 applies for the smectitic clays (bioactive: 700.18; non-bioactive 700.20).

Turning now to the bioactivity of the synthetic samples (Suppl file 1 and Fig. 2), Melos smectite + B (sample 4) and kaolinite + B (sample 5) are the most effective synthetics against both *P. aeruginosa* and against *S. aureus*, with (4) being better than (5) re the latter. Melos kaolinite + Al (7) is equally effective. Melos smectite + Fe (15) and Melos kaolinite + Fe (14) are not bioactive against either Gram-negative and Gram-positive bacteria. Melos smectite + Ti (10) and kaolinite + Ti (9) are also non-active and neither is Al-spiked Melos smectite (6). Solutions of reagent-grade boric acid (2) and reagent grade aluminium sulphate (8) are also included here for comparison. As already mentioned the most effective antibacterial is sample 3, natural alunogen, from SE Melos, which is not a clay.

INSERT FIG.2

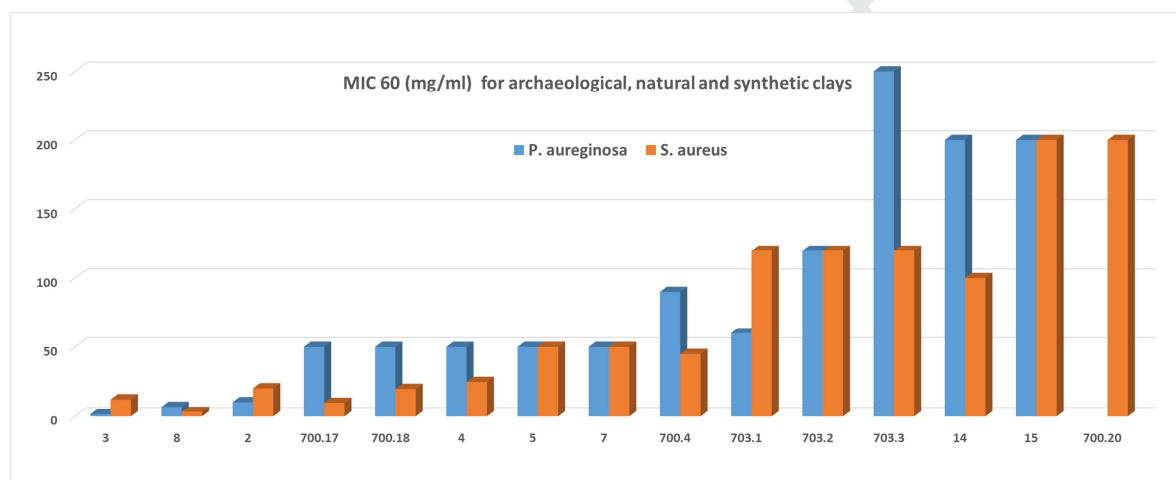


Fig. 2 Illustration of relative bioactivity between archaeological MEs, natural (700.19, 700.20) and synthetic samples consisting of kaolinitic/smectitic clays spiked with Al, B, Ti and Fe. The absence of a bar indicates lack of bioactivity. Blue denotes *P. aeruginosa* and Red *S. aureus*.

In summary, the most active samples against *both* pathogens are the two LEs, 700.17, 700.18, as well as the two boron-rich synthetic samples (4 and 5) and the aluminium-rich kaolinite (7). It is not clear why this sample is bioactive while the aluminium-rich smectite (6) is not. As for clays spiked with Ti (9 and 10) or Fe (14 or 15) they were inactive. What transpires from the above results is that smectitic clays can be *both* bioactive (700.18) *and* non bioactive (700.20). Equally, kaolinitic clays can be *both* bioactive (700.17) *and* non bioactive (700.19). It follows that bulk mineralogy does *not* drive bioactivity. Referring back to the graphical abstract, the next step is to investigate in detail the chemical make-up of the leachate of the bioactive MEs and synthetics and the range of trace elements associated with each group. Suffice it to say that the graphical abstract has no prescribed sequence in the analysis. It is the combined results from all techniques and how one feeds into the other that help shape our understanding of the antibacterial efficacy of these clays.

3.2. The chemical composition of the leachates of the bioactive MEs

Table 2 compares the chemical composition of the leachates of the six MEs, the two natural clays from Lemnos (700.19 and 700.20) and the two from Melos (900.9 and 933) and three synthetics (4, 5 and 7). The range of parameters appears at first bewildering and comparisons on an element by element basis seems to confuse rather simplify the picture.

The chemical composition of the six archaeological MEs, the four naturals (700.19, 700.20, 900.9 and 933) and the bioactive synthetics (4, 5 and 7) is shown in Table 2. Focusing on the three bioactive synthetic samples above and the two bioactive archaeological LEs (700.17 and 700.18) we show that 700.17 is more abundant in Al, Ti, V, Cr, Cu, Sr and Ba than, for example 900.9. The latter is deficient in Al and thus it is not expected to be bioactive. It is only with enhanced amounts of (spiking with) B and Al that Melos kaolinite can match the bioactivity of archaeological LE 700.17. On the other hand, comparison of smectitic LE 700.18 with the natural Melos smectite 933, suggests that this latter clay cannot be bioactive, either, unless spiked with Al given the small concentrations in that element as well as, Ti, V, Cr and Cu. Regarding the natural Lemnos clays, 700.19 and 700.20, although rich in Ti, V, Mn and Ba, it has been demonstrated that they are not bioactive (Fig. 2).

Turning now to the SEs, the B content (in ppb) in the leachates is higher than that of the LEs and yet the SE with the highest boron (703.2) is not antibacterial. In the case of 703.1, the Al content of the leachate is very low and yet this particular ME is antibacterial (against *P. aeruginosa*). Ti concentration is the highest in 703.2 and 700.19 and yet none of these two samples are bioactive. Interestingly sample 703.2, the richest in iron oxide (Table 1) has a very low Fe content in the leachate, compared to 700.17 and 700.18. Finally, Melos smectite spiked with Al (6) is non-bioactive despite having similar or near-similar Al contents as the bioactive MEs. This may be due to the fact that Al is precipitated due to the buffering capacity of smectite.

In summary, there is no obvious correlation between elemental composition of the leachate and bioactivity, and in reference to the elements investigated in detail here, namely Ti, Al, B, Fe. Samples with the above elements, whether MEs, naturals or synthetics, can be *either* bioactive or non-bioactive.

INSERT TABLE 2

Table 2 ICP-MS data for the leachates of MEs, natural Lemnos clays (700.19 and 700.20) and synthetic clays (4, 5, 7): bdl= below detection ; adl= above detection limit. Concentraions of the major elements (Si, Al, Mg, Fe, Ca, Na and K) are in ppm. The remaining elements are in ppb.

	703.1	703.2	703.3	700.4	700.17	700.18	4	5	7	900.9	933	700.19	700.20
Na	6	6	6	1	2	3	adl	9	5	adl	17	nd	nd
Mg	12	2	4	59	1	10	22	14	3	22	1	nd	nd
Al	2	24	2	4	4	4	28	33	adl	0	1	nd	nd
Si	2	11	1	1	2	1	1	3	bdl	1	7	nd	nd
K	10	5	3	2	9	4	13	8	1	14	3	nd	nd
Ca	8	4	7	89	3	6	7	532	5	8	2	nd	nd
Fe	1	1	0	1	18	14	0	5	0	6	0	nd	nd

Li	40	42	20	33	24	2	4	18	7	1	8	6	76
B	35	52	14	7	16	12	bdl	6	2	35	20	5	12
Ti	41	1260	448	115	216	827	1	47	5	1	48	1478	485
V	bdl	8	2	26	51	71	bdl	bdl	bdl	bdl	3	95	49
Cr	2	1	1	13	38	7	bdl	bdl	4	bdl	1	32	62
Mn	1099	72	14	43	65	258	4	2	27	5	bdl	979	291
Co	3	1	0	bdl	1	4	bdl	2	bdl	bdl	bdl	14	9
Ni	34	38	14	bdl	4	9	4	19	24	5	9	13	82
Cu	15	18	20	176	17	31	8	2	15	8	7	28	14
Zn	324	543	119	3	14	29	26	83	452	36	6	34	35
As	bdl	bdl	12	3	77	5	bdl	bdl	bdl	bdl	bdl	5	0
Se	bdl	bdl	bdl	bdl	bdl	bdl	bdl	bdl	bdl	bdl	18	nd	nd
Rb	5	8	5	16	52	25	4	103	1	4	8	29	38
Sr	32	51	45	323	52	25	209	706	32	214	10	301	92
Y	1	bdl	1	bdl	bdl	bdl	bdl	1	bdl	bdl	bdl	nd	nd
Mo	4	6	2	bdl	bdl	bdl	4	2	1	4	1	nd	nd
Cd	bdl	bdl	bdl	bdl	bdl	bdl	bdl	bdl	bdl	bdl	bdl	nd	nd
Sn	bdl	bdl	bdl	bdl	bdl	bdl	bdl	bdl	bdl	bdl	bdl	nd	nd
Sb	2	2	2	bdl	bdl	bdl	0	2	2	0	bdl	nd	nd
Cs	5	11	6	2	12	4	4	22	3	4	5	1	2
Ba	31	27	60	53	136	629	71	13	51	73	bdl	865	78
Hg	11	10	0	bdl	bdl	bdl	bdl	bdl	bdl	bdl	bdl	nd	nd
Pb	bdl	1	7	17	10	40	7	bdl	0	7	1	33	8
U	0	0	0	bdl	bdl	bdl	8	3	0	0	0	nd	nd

509

510 *3.5.Nanoparticle analysis*

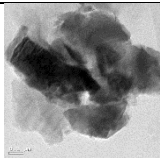
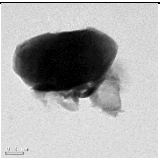
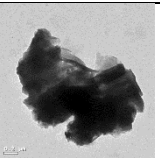
511 TEM/EDX data of the fine fractions of the bioactive samples (700.17, 700.18) are
512 shown in Fig. 3. For the rest of the non-bioactive samples see and suppl files 2a-b.
513 The particles of 700.17a and c are characterized by the presence of anatase (TiO₂
514 polymorph) even though it was not detected in the bulk sample (Table 1). The
515 analysis of 700.17b is consistent with silicates and clays containing Fe and low levels
516 of titanium oxide, and may represent a mixture of phases. The cobalt and vanadium
517 present are also seen in the ICP-MS data (Table 2) and may be associated with
518 titanium oxide minerals.

519

520 **INSERT FIG. 3**521 **Fig. 3** Nanoparticles of bioactive LEs

522

	700.17a	700.17b	700.17c	700.18a	700.18b	700.18c
Na				0.34		
Mg				0.52		0.53
Al	0.91	1.27	0.25	17.28	1	12.38
Si	2.85	38.75	0.37	7.54	47.46	7.61
P				6.18		1.8
S				6.85		7.51
K		0.19		2.19	0.13	4.01
Cl						0.31
Ca				3.59	0.09	0.62
Ti	57.13	0.13	50.83			15.44

			
700.18a (>1000nm)	700.18b 1240nm	700.18c (1560nm)	
			Analysis of nanosized particles for Lemnos medicinal earths (in %). Blanks denote absence

The particles from 700.18 are of three different compositions: the analysis of particle 700.18c is consistent with a mixture of clay minerals and anatase, with cobalt and vanadium being present. The XRD analysis (Table 1) did not show any anatase in the bulk material, but the leachate showed high Ti levels (Table 2). In contrast, the composition of 700.18b is consistent with the presence of quartz and illite/mica and low levels of clay minerals, in line with the XRD data for the bulk material (Table 1). The composition of 700.18a is variable, with a wide range of elements present. The levels of phosphorous and sulfur may indicate some organic material. There also appears to be clay minerals present. Suppl files 2 show TEM images and EDAX table of data for the non-bioactive samples, whether MEs (SEs) or naturals (Lemnos natural clays).

In summary, the nanosized fractions of 700.17 and 700.18 reflect their bulk compositions, but they are not informative of the difference in bioactivity between these two samples and the non-bioactive samples.

Regarding the particle size analysis data, the average diameters of the two archaeological samples is 200nm (700.17) and 309nm (700.18) (see suppl file 2c); their large standard deviations indicate highly variable particle sizes. The size variation in these samples is attributed to the coexistence of clay and non-clay mineral nanoparticles (quartz, anatase, carbonates, Fe-oxyhydroxides) which are expected to have different sizes.

3.6. The organic load: DNA community analysis

The quantities of extracted DNA from all samples were relatively low (< 2ng/ul), or < 1.0 ng/ul, of starting material (Table 3); for example, 703.2 and 703.3 yielded 1.2 and 1.5 ng/ul, of DNA material, respectively. Although these values fell below the range for quantification (i.e. [DNA] are not significantly greater than zero), bacterial signals were noticed following PCR amplifications. Similar PCR screens, using cyanobacterial/chloroplast 16S-rRNA gene-specific primers and presumed universal primers for fungus (Hadziavdic et al., 2014), did not reveal any strong signals (except trace chlorophyll/chloroplast in 700.18). As such, metataxonomic analysis of the microbial communities initially focused on the bacteria. The results are presented in Table 3 and in more detail in Suppl file 3.

INSERT TABLE 3

Table 3 Bacteria identified from DNA extracted from four samples, based on 16S-rRNA meta-taxonomic analysis; their relative abundances are denoted, as % of total. Superscripts refer to the bacterial genus present within each sample.

Bacterial phylum	700.17 ¹	700.18 ²	700.19 ³	703.1 ⁴	Genus
α-proteobacteria	44.6	55.8	0	30	<i>Bradyrhizobium</i> ^{1,2} , <i>Sphingomonas</i> ¹ , <i>Acidiphilum</i> ⁴ , <i>Brevundimonas</i> ¹ , <i>Devosia</i> ¹ , <i>Microvirga</i> ⁴
β-proteobacteria	41.7	4.7	0	0	<i>Achromobacter</i> ¹ , <i>Comamonas</i> ²
γ-proteobacteria	4.4	2.3	5	0	<i>Acinetobacter</i> ¹ , <i>Pseudomonas</i> ² , <i>Aeromonas</i> ³
ε-proteobacteria	0	2.3	0	0	<i>Acrobacter</i> ²
Actinobacteria	0	2.3	0	0	<i>Gaiella</i> ²
Bacteroidetes	2.2	18.6	0	0	<i>Flavobacterium</i> ^{1,2}
Chlorobi	0	0	15	0	<i>Chlorobium</i> ³
Chloroflexi	0.7	0	5	0	<i>Anaerolinea</i> ^{1,3}
Cyanobacterium	0	2.3	0	0	<i>GpXIII</i> ²
Firmicutes	0	2.3	5	0	<i>Staphylococcus</i> ² , <i>Clostridium</i> ³
Fusobacteria	0	0	5	0	<i>Fusobacteria</i> ³
Thermotogae	2.2	0	10	0	<i>Mesoaciditoga</i> ^{1,3}
Verrucomicrobia	0	0	0	10	<i>Spartobacteria</i> ⁴
Unknown	4.2	9.4	55	60	

However, subsequent PCR-primer development and confirmatory DNA sequencing successfully detected DNA signatures related to the fungal Trichocomaceae family (Ascomycota (division), Eurotiomycetes (class), and Eurotiales (order)) with *Talaromyces*, or related, DNA often showing closest resemblance. The following concentrations were found based on qPCR: 700.18 (approx. 10² gene copies/mg) and 700.17 (approx. 10¹ gene copies/mg). 703.1, which appeared to have stronger DNA sequence bias towards *Aspergillus* sp. than *Talaromyces* sp., had approx. 10³ gene copies/mg; signals in 703.2 were below detection.

To confirm the quality of PCR detection of the *Talaromyces* and related fungus products were sent for DNA sequencing (Eurofins Scientific) and compared via BLASTn algorithms to GenBank (National Centre for Biotechnology). All results were represented closely-related clades within the Eurotiales phylogenetic order, particularly: *Talaromyces*, *Penicillium* and *Aspergillus*. While it remains difficult to recognise specific microorganisms from short DNA sequence from a single locus, there were specific patterns in that could be discerned. Sample 700.17 showed the strongest evidences of specific *Talaromyces* species, with commonalities among the bi-directional reads, while the possibility for *Penicillium* sp. and *Aspergillus* sp. is still present. Sample 700.18 was clearly represented by either *Talaromyces* or *Penicillium*; both genera are teleomorphs, and *Talaromyces* sp. have historically been included within the *Penicillium* nomenclature; as such organisms in this clade may be mentioned in the literature interchangeably (Yilmaz et al., 2014; Frisvad, 2015), which further complicates recognition. Sample 703.1 showed greater alignments with *Aspergillus* and different *Penicillium* sp., and sample 703.2 had minimal DNA and had the least conclusive data (with greater mis-alignment of the sequences). It should be noted that the presence of a genus does not suggest antibiotic production, rather the possibility of micro-organisms that may produce exometabolites.

4. Discussion

4.1 Bioactivity - the contribution of the inorganic component (in reference to elements Ti, Fe, Al and B as leachates or nanoparticles)

A total of 21 samples consisting of six archaeological medicinal clays (700.4, 700.17, 700.18, 703.1, 703.2, 703.3), four natural clays (700.19, 700.20, 900.9, 933), eight synthetic clays (4,5,6,7,9,10,14,15) deriving from the spiking of two natural clays (900.9, 933) with B, Al, Ti, Fe and three (non-clay) controls (3, 2, 8) were examined mineralogically, in bulk and for their nanoparticle composition, chemically, and also tested for bioactivity against *P. aeruginosa* and *S. aureus* following a method illustrated in the graphical abstract.

Of a total of eighteen samples examined, only archaeological samples 700.17, 700.18 and synthetic samples 4 (smectite spiked with B), 5 (kaolinite spiked with B), and 7 (kaolinite spiked with Al) displayed antibacterial action against both Gram-positive and Gram-negative pathogens. For the purposes of this discussion we consider bioactive the samples which display MIC₆₀ <50mg/ml. Natural clays, while not naturally bioactive, were rendered bioactive with the addition of B and or Al. However the archaeological samples 700.17 and 700.18 did not contain any meaningful concentrations of these two elements. Therefore the question arises: why are these two samples bioactive? Before addressing this issue we turn to a brief review of the literature regarding antimicrobial clays and the mechanisms proposed, so far, for their antimicrobial activity.

Various researchers have attributed the bioactivity of the antimicrobial clays they have investigated to different reasons: a) to the toxic influence of heavy metals such as Cu, Zn and Ni (Otto et al., 2010); b) to the role of nanosized accessory Fe²⁺-bearing phases, that might generate reactive oxygen species (Morrison et al. 2016; Williams 2017); c) to the presence of soluble Al³⁺ (Londono et al., 2016); finally, d) to the existence of Fe²⁺-atoms in active unsatisfied bonds at clay mineral edges which

might form hydroxide radicals upon oxidation (Wang et al., 2007). These studies have focused on specific ions and heavy metals, but they did not necessarily offer definitive answers for clay antimicrobial activity. For example, when these proposed mechanisms were applied to clays other than those involved in the studies (for example Fe-saponite), they yielded contradictory results (Zarate-Reyes et al., 2018).

Interestingly, none of the above studies has acknowledged or sought to investigate the presence and contribution of an organic load. Indeed, all researchers have used clays which have been sterilized in the autoclave, prior to any detailed investigation, thus destroying any microorganisms within. Here we examine both the nature of the microbiome and the contribution of each one of the elements already discussed in the above studies i.e. Al, Fe, Ti and B; also the role of some transition metals in influencing the bioactivity of the archaeological medicinal earths. Since the toxic influence of transition metals has already been discussed (Otto et al., 2010; Otto & Heydel, 2013) we note that, although largely present in the SE samples, these samples displayed low or no bioactivity. Therefore we conclude that transition metals did not have a role to play in driving the bioactivity of the two LEs.

Titanium

Recent work has shown that TiO₂ nanoparticles readily produce reactive oxygen species (ROS) which are toxic to the membrane cells of bacteria, when exposed to visible light, especially in arid environments (Georgiou et al., 2015). The generated ROS will be rapidly converted to H₂O₂ upon contact with water by dismutation (i.e. simultaneous oxidation and reduction) (Halliwell and Gutteridge, 2015). In this case, the antibacterial activity will be controlled firstly by the abundance of TiO₂ reactive nanoparticles in the leachate and secondly by the probability of contact and reaction between the generated H₂O₂ and the bacterial cells. In the present study, although titanium is present in both MEs and is considerably higher in SEs (Table 2). However, TiO₂ nanoparticles were found primarily in 700.17 and 700.18, the bioactive LEs (Fig. 3) and not in the SEs despite the presence of c.4% anatase (TiO₂ polymorph) in 703.2.

The two LE samples are indeed the more bioactive, thus corroborating the contribution to bioactivity of TiO₂ nanoparticles rather than their ionic counterparts. Equally the synthetic control samples of kaolinite and smectite (9 and 10) (Table 2) with 20% anatase nanoparticles did not yield leachates with, as anticipated, antibacterial properties. This may be due to aggregation of TiO₂ nanoparticles to larger particles, which decreased their activity. Therefore, we suggest that the potential antibacterial role of TiO₂ nanoparticles should be examined carefully. The formation of ROS as mentioned above (Georgiou et al., 2015), would have necessitated a photochemical reaction and therefore is not relevant to the present study. We conclude that the TiO₂ nanoparticles in 700.17 and 700.18 may play a small role in the samples' bioactivity but their overall effect would depend on the amounts present.

Fe-oxides

The LE and the SE samples do not contain traceable amounts of Fe²⁺-bearing phases, such as pyrite, which might have contributed to their antibacterial potential; this would have taken place via generation of ROS, causing detrimental effect on bacteria

through oxidative stress, penetration of the cell wall and destruction of cellular components (Cagnasso et al., 2010; Morrison et al., 2016; Williams, 2017). LEs 700.17 and 700.18 do contain Fe⁺ above the rest of the samples. However, the Fe-content of the nanoparticles present in the leachates of the LEs is considerably lower than that of their counterparts in the SEs, with the exception of 703.1; which showed low bioactivity. When natural clays were spiked with Fe (oxides/ oxyhydroxides) hematite/goethite, (samples 14, 15), they showed no bioactivity. We conclude that Fe⁺ in 700.17 and 700.18 might play a small role in the samples' bioactivity.

Aluminium and Boron

Aluminium originating from the dissolution of clay minerals and/or aluminium sulphates in the leachates is toxic to cells and might trigger antibacterial action (e.g. Londono et al., 2016; Williams, 2017). Similarly, boron has been reported to be antibacterial (Photos-Jones et al., 2015). However, Al and B concentrations in the leachates of 700.17 and 700.18 were very low compared to the rest of samples which were not bioactive (Table 2). By contrast the Melos kaolinite spiked with alum (sample 7, Fig. 2) and especially the Melos alunogen (sample 3, Fig. 2) showed antibacterial activity, particularly the latter. Melos kaolinite and smectite spiked with Boron are also equally antibacterial (Fig. 2). We conclude that Al and B are not driving the bioactivity of 700.17 and 700.18.

Nanoparticle active edges

The possible contribution of the active nanoparticle edges on the antibacterial/bacteriostatic activity of the leachates should also be considered. All leachates contain phyllosilicates, mainly illite, kaolinite and smectite along with anatase and dolomite. Carbonates are not considered to have antibacterial properties and the possible role of TiO₂-polymorphs such as anatase was considered previously. Therefore, in this section we focus on the possible influence of the nanoparticle active edges of clay minerals. Smectite edges have been shown to have oxidative capacity due to formation of superoxide oxygen radical by chemisorption of oxygen atoms in crystallite edges (Thompson and Moll, 1973), caused by simultaneous oxidation of structural Fe²⁺, which have been shown to have antibacterial activity (Wang et al., 2007).

The oxidative capacity of kaolinite and illite has not been evidenced so far. In the present study the octahedral Fe in smectites is considered to be in Fe³⁺ form, which is not known to contribute to bioactivity. However, the formation of superoxide oxygen radicals in smectite edges might be controlled by particle size as well (Gournis et al., 2002). In this aspect the smectite nanoparticles present in the leachates might also, to some extent, contribute to the observed bioactivity of the LE samples. Nevertheless, their importance should not be overemphasized. This because although illite, the main phyllosilicate which might contain Fe²⁺, a potential source of superoxide oxygen radicals nanoparticles, is present in both LE and SE earths, only the LE ones are bioactive.

In conclusion, the clay nanoparticles present in the leachates of LE and SE samples do not seem to be the dominant factors driving bioactivity. In the case of the synthetic control samples bioactivity is controlled by the chemicals added, namely H₃BO₃ and Al-sulfate and to a lesser degree by metals released such as Zn. The role of Fe²⁺-

bearing phases and active oxides such as TiO_2 , which may produce superoxide oxygen radicals during oxidation via Fenton-like reactions, seems also to be limited.

4.2 . Bioactivity – the contribution of the organic component

Most DNA signatures represented soil bacteria (Table 3); some species are recognised as producers of antibacterial compounds. For example, *Bradyrhizobium* (alpha-proteobacteria) found in bioactive 700.17 and 700.18 are bacteria commonly associated with nitrogen-fixation in soils. They excrete porphyrins, which act as metal (M^{+2}) chelators and may become antibiotic precursors. 700.17 also contains abundant *Achromobacter*, which are known hydrocarbon degraders that may produce intermediary compounds with greater toxicity.

Further to the above, rhizobial bacteria, *Sphingomonas* and sulfur-related bacteria (e.g. *Chlorobium*), naturally affect sulfur compounds which may increase solubility of metals/metalloids potentially toxic to bacteria. However, since the concentrations of these metals /metalloids in the SE and LE leachates (Table 3) are low, their contribution to antibacterial activity must be considered to be limited. Moreover, *Pseudomonas*, *Comamonadaceae*, *Arcobacteria*, *Aeromonas*, and *Achromobacter* contain species related to pathogenesis although they may also be considered environmental. It is concluded that both bioactive and non-bioactive MEs.

Apart from bacteria genetic analysis was also conducted on fungi (based on their analogous 18S-rRNA gene). Of greatest interest was the presence, within samples 700.17 and 700.18, of Trichocomaceae (Eurotiales) fungi. Following genetic analysis we discovered by in-silico analysis (via RDP and NCBI databases for genetic sequences) that the “universal” primers for detecting fungus (e.g. Hadziavdic et al., 2014), while able to capture many signatures for such communities, they would not have recognized the 18S-rRNA from *Talaromyces*; as a result new genetic primers were developed (see Methods section).

Talaromyces (and *Penicillium*) are saprotrophic organisms and contribute to the spoilage of carbohydrate-rich foodstuff. But they are notorious producers of exometabolites (Yilmaz et al., 2014; Frisvad, 2015), including antibiotics (e.g. penicillin), and highly tolerant of extreme conditions (Samson, 2016). Both *Talaromyces* are expected to form biofilms (on surface), when low on nutrients or stressed, or be plankton-like (i.e., floating) when “feasting”. Being saprobes, living off dead or decaying organic material, they will tend to remain at/near clay sediments; the latter may help adsorb nutrients. They do not need light and will respire CO_2 .

Another reason that the evidence for *Talaromyces* attracted our attention was the recent publication by Pangging et al. (2019) who discovered that a new isolate, *Talaromyces apiculatus* from Korean soil, produced bioanthracene. The detection of bioanthracene has already been highlighted by Photos-Jones et al. (2017) and in association with 700.18, the only one of the three LEs analysed at the time.

Although acknowledged, the specific mention of bioanthracene production by *Talaromyces* remains, nevertheless, rather limited in literature (e.g. Yilmaz et al., 2014; Panggling et al., 2019; Gao et al., 2013) with *T. apiculatus* being the one most frequently mentioned. However, *Talaromyces* produce other bioactive compounds

summarized by Nicoletti and Trincone (2016) and Yilmaz et al., (2014) with beneficial and detrimental health-related effects depending on exometabolite. Bioanthracene has been found to be bioactive against the parasite *Plasmodium* and potentially against bacteria as well (Saepua et al., 2018; Jaturapat et al., 2001).

Bioanthracene aside, *Talaromyces* sp. and some *Penicillium* sp. have also gained their notoriety for their ability to produce polyketide-based pigments, many of which also carry antibacterial properties (Caro et al., 2016; Rao et al., 2017). Conditions for their production and excretion of exo-metabolites have been found to be environmentally based, for example a source of carbohydrate, pH, temperature and geochemical conditions in their surroundings (e.g. presence of potentially toxic elements, which promote extra-cellular excretions) (Mendez et al., 2011; Santos-Ebinuma et al., 2013); further, biotechnological efforts continue to research optimum production for the food (e.g. Defosse, 2006) and textile industries as dye producers (Chadni et al., 2017).

5. Concluding remarks

Over the last few years we have been testing the bioactivity of archaeological medicinal earths first, because it is a relatively straight forward parameter to measure (their reported use as ‘antidotes to poison’ is clearly too generic a description to begin to address experimentally and in a meaningful way) and second, on the grounds that they *might prove to be* useful antibacterials. This paper provides a quantitative assessment of the bioactivity of six samples of medicinal earths from the collection of the Pharmacy Museum of the University of Basel.

Of the six MEs only two LEs (700.17 and 700.18) are bioactive against one Gram-positive and one Gram-negative bacteria, while the third (700.4) is bioactive against Gram-positive only and one SE (703.1) is mildly antibacterial against Gram-negative only. Bioactivity, under the conditions set out in this paper was defined as having an $MIC_{60} < 50\text{mg/ml}$.

The bioactivities of the leachates of 700.17 and 700.18 are comparable with synthetic Melos smectite and kaolinite spiked with Boron and also Melos kaolinite spiked with Al. We note that 700.17 and 700.18 are Al and B deficient and so they cannot be bioactive on account of these two elements.

Looking at other reasons for their bioactivity and more specifically into their microbiomial load, we note that 700.17 and 700.18 contain, with certainty, the fungus *Talaromyces* spp. A greater certainty for the fungus *Aspergillus* (another member of the phylogenetic clade) and a different *Penicillium* were suggested for 703.1 which was mildly antibacterial against *P. aeruginosa*, only. We conclude that the fungal, rather than the bacterial load, is the key driver imparting bioactivity to the three MEs (700.17, 700.18 and to a lesser extent in 703.1)

Based on a protocol of analysis (illustrated in the graphic abstract), we suggest that antibacterial activity of archaeological MEs seems to derive primarily from the clays’ organic load; the contribution of TiO₂ nanoparticles, if in sufficient numbers might have also a role to play. We do not know how the LEs examined here acquired their specific organic load, although we acknowledge that *Talaromyces* and *Penicillium* are

ubiquitous. We conclude such that clays with a fungal or bacterial load might be worth investigating further as potentially serious antibacterial agents.

Acknowledgements

The authors are indebted to Mrs Corinne Eichenberger and the director and Trustees of the Pharmacy Museum of the University of Basel for making the archaeological samples available for analysis. Also Ms N Andriopoulou, University of Crete, for the preparation of synthetic clays and the unknown reviewers for their constructive queries and comments.

Funding

Funding has been provided by: Wellcome Trust (Seed Award in the Humanities and Social Sciences (201676/Z/ 16/Z); and NERC-FENAC award (FENAC/2015/11/07). The work is part of a larger study into Greco–Roman antimicrobial minerals. Principal investigator: E. Photos-Jones.

Authors' contributions

GEC- responsible for mineralogical /elemental analysis and interpretation, author of relevant sections.

CK- responsible for DNA sequencing and interpretation of ME microbiome, author of relevant sections.

DV and IG - responsible for MIC measurements, interpretation of antibacterial activity and authorship of relevant section.

CE and EVJ- responsible for nanoparticle analysis, interpretation and authorship of relevant section.

EPJ - initiator/coordinator of project and responsible for overall preparation and manuscript submission and resubmission after reviewing.

References

Andrews J.M., 2001. Determination of minimum inhibitory concentrations. *J. Antimicrob. Chemother.* 48, Suppl.S1, 5-16.

Anderson, J.U., 1963. An improved pretreatment for mineralogical analysis of samples containing organic matter. *Clays and Clay Minerals* 10, 380--387.

Brock, A.J., 1929. *Greek medicine being extracts illustrative of medical writers from Hippocrates to Galen.* Dent, London.

Cagnasso, M., Boero, V., Franchini, M.A., Chorover, J., 2010. ATR-FTIR studies of phospholipid vesicle interactions with α -FeOOH and α -Fe₂O₃ surfaces. *Colloids Surfaces B. Biointerfaces* 76, 456–467. [https://doi: 10.1016/j.colsurfb.2009.12.005](https://doi.org/10.1016/j.colsurfb.2009.12.005).

Caro, Y., Venkatachalam, M., Lebeau, J., Fouillaud, M., Defosse, L., 2016. Pigments and colorants from filamentous fungi, in: Merillon, J-M., Ramawat, K.G.

- (Eds.), *Fungal Metabolites*, Reference Series in Phytochemistry. Switzerland, Springer International Publishing. https://doi.org/10.1007/978-3-319-25001-4_26.
- Chadni, Z., Rahaman, M.H., Jerin, I., Hoque, K.M.F., Reza, M.A., 2017. Extraction and optimisation of red pigment production as secondary metabolites from *Talaromyces verruculosus* and its potential use in textile industries. *J. Fungal Biol.* 8(1), 48-57.
- Cole, J.R., Wang, Q., Fish, J.A., Chai, B., McGarrell, D.M., Sun, Y., Brown, C.T., Porras-Alfaro, A., Kuske, C.R., Tiedje, J.M., 2014. Ribosomal Database Project: data and tools for high throughput rRNA analysis. *Nucl. Acids Res.* 42(Database issue): D633-D642; <https://doi.org/10.1093/nar/gkt1244>.
- Defosse, L., 2006. Microbial production of food grade pigments. *Food Technol. Biotechnol.* 44, 313-21.
- Dannenfeldt, K.H., 1984. The introduction of a new sixteenth century drug: Terra Silesiaca. *Medical History* 28, 174-188.
- Duffin, C.J., 2013. Some early eighteenth century geological *Materia Medica*. In Duffin, C. J., Moody, R. T. J. & Gardner-Thorpe, C. (eds) 2013. *A History of Geology and Medicine*. Geological Society, London, Special Publications, **375**, 209-233.
- Frisvad, J.C., 2015. Taxonomy, chemodiversity, and chemoconsistency of *Aspergillus*, *Penicillium* and *Talaromyces* species. *Front. Microbiol.* 12. <https://doi.org/10.3389/fmicb.2014.00773>.
- Gao, H., Zhou, L., Li, D., Gu, Q., Zhu, T.J., 2013. New cytotoxic metabolites from the marine-derived fungus *Penicillium* sp. ZLN29. *Helv. Chim. Acta* 96, 51-19.
- Georgiou, C.D., Sun, H., McKay, C.P., Grintzalis, K., Papapostolou, I., Zisimopoulos, D., Zhang, G., Koutsopoulou, E., Christidis G. and Margiolaki, I., 2015. Detection of photochemical superoxide radicals in chemically reactive desert soils. *Nature Communications*. <https://doi.org/10.1038/ncomms8100>.
- Gournis, D., Karakassides, M.A., Petrides, D., 2002. Formation of hydroxyl radicals catalyzed by clay surfaces. *Physics and Chemistry of Minerals* 29, 155-158.
- Hall, A.J., Photos-Jones, E. 2008. Accessing past beliefs and practices: the case of Lemnian Earth. *Archaeometry* 50, 1034–1049.
- Halliwell, B., Gutteridge, C.M.J., 2015. *Free Radicals in Biology and Medicine* 3rd ed.. Oxford, Oxford University Press.
- Hadziavdic, K., Lekang K., Jonassen, I., Thompson, E.M., Troedsson, C., 2014. Characterization of the 18S rRNA Gene for Designing Universal Eukaryote Specific Primer. *PLOS*. <https://doi.org/10.1371/journal.pone.0087624>.

- Hardy, A., Rollinson, G., 2016. A chemical study of a 'Terra Sigillata' medicinal tablet from a late 17th century Italian medicine chest. *Pharmaceutical Historian* 46(1), 2-7.
- Hasluck, F.W., 1909–1910. Terra Lemnia. *Annual British School at Athens XVI*, 220–231.
- Hasluck, F.W., Hasluck, M.M., 1929. *Christianity and Islam under the Sultans. Terra Lemnia, II*, Oxford, Clarendon Press.
- Haydel S.E., Remenih C.M., Williams L.B., 2008. Broad-spectrum in vitro antibacterial activities of clay minerals against antibiotic-susceptible and antibiotic-resistant bacterial pathogens. *J Antimicrob Chemother* 61:353–361 . doi: 10.1093/jac/dkm468
- Jaturapat, A., Isaka, M., Hywel-Jones, N.L., Lertwerawat, Y., Kamchonwongpaisan, S., Kirtikara, K., Tanticharoen, M., Thebtaranonth, Y., 2001. Bioanthracenes from the insect pathogenic fungus *Cordyceps pseudomilitaris* BCC1620. I. Taxonomy, fermentation, isolate, and antimalarial activity. *J. Antibiot.* 54, 29-35.
- Keller, N.P., 2019. Fungal secondary metabolism: regulation, function and drug discovery. *Nature Rev. Microbiol.* 17, 167-180.
- Knapp, C.W., Graham, D.W., 2004. Development of alternate ssh-rRNA probing strategies for characterizing aquatic communities. *J. Microbiol. Meth.* 56(3), 323-330. [https://doi: 10.1016/j.mimet.2003.10.017](https://doi.org/10.1016/j.mimet.2003.10.017).
- Locatelli, F.M., Goo, K-S., Ulanova, U., 2016. Effects of trace metal ions on secondary metabolism and the morphological development of streptomycetes. *Metallomics* 8, 469. [https://doi 10.1039/c5mt00324e](https://doi.org/10.1039/c5mt00324e).
- Londono, S.C., Hartnett, H.E., Williams, L.B., 2016. Unraveling the antibacterial mode of action of a clay from the Colombian Amazon. *Environ. Geochem. Health* 38, 363–379. [https://doi: 10.1007/s10653-015-9723-y](https://doi.org/10.1007/s10653-015-9723-y).
- MacGregor, A., 2013. Medicinal terra sigillata: a historical, geographical and typological review, in: Duffin, C.J., Moody, R.T.J., Gardner-Thorpe, C. (Eds.), *A History of Geology and Medicine*. London, Geological Society, Special Publications 375, 113–136, <https://doi.org/10.1144/SP375.29>.
- Macheleidt, J., Mattern, D.J., Fischer, I., Netzker, T., Weber, I., Schroeckh, V., Valiante, V., Brakhage, A.A., 2016. Regulation and role of fungal secondary metabolites. *Ann. Rev. Genetics* 50, 371-392.
- Manaia C.M., Macedo, G., Fatta-Kassinos, D., Nunes, O.,C., 2016. Antibiotic resistance in urban aquatic environments: can it be controlled? *Appl Microbiol Biotechnol* 100:1543–1557 . doi: 10.1007/s00253-015-7202-0

- Maidak B.L., Cole, J.R., Lilburn, T.G., Parker, C.T., Saxman, R., Farris, R.J., Garrity, G.M., Olsen, G.L., Schmidt, T.M., Tiedje, T.G., 2001, The RDP-II (Ribosomal Database Project). *Nucl Acid Rs* 29(1): 173
- Medina, A., Schmidt-Heydt, M., Rodríguez, A., Parra, R., Geisen, R., Magan, N., 2015. Impacts of environmental stress on growth, secondary metabolite biosynthetic gene clusters and metabolite production of xerotolerant/xerophilic fungi. *Current Genetics* 61(3), 325-34. [https://doi: 10.1007/s00294-014-0455-9](https://doi.org/10.1007/s00294-014-0455-9).
- Mendez, A., Perez, C., Montanez, J.C., Martinez, G., Aguilar, C.N., 2011. Red pigment production by *Penicillium purpurogenum* GH2 is influenced by pH and temperature. *Biomed. Biotechnol.* 12, 961-8.
- Morrison, K.D., Misra, R., Williams, L.B., 2016. Unearthing the Antibacterial Mechanism of Medicinal Clay: A Geochemical Approach to Combating Antibiotic Resistance *Scientific Reports*, DOI: 10.1038/srep19043
- Nicoletti, R., Trincone, A., 2016. Bioactive compounds produced by strains of *Penicillium* and *Talaromyces* of marine origin. *Mar. Drugs* 14: 37
- Nutton, V., 2004. *Ancient Medicine*. London ; New York : Routledge
- Otto, C.C., Cunningham, T.M., Hansen, M.R., Haydel, S.E., 2010. Effects of antibacterial mineral leachates on the cellular ultrastructure, morphology, and membrane integrity of *Escherichia coli* and methicillin-resistant *Staphylococcus aureus*. *Ann. Clin. Microbiol. Antimicrob.* 9:26. doi: 10.1186/1476-0711-9-26.
- Otto, C.C., Haydel, S.E., 2013. Exchangeable Ions Are Responsible for the In Vitro Antibacterial Properties of Natural Clay Mixtures. *PLoS One* 8, 1–9. [https:// doi: 10.1371/journal.pone.0064068](https://doi.org/10.1371/journal.pone.0064068).
- Pettit, R.K., 2011. Small-molecule elicitation of microbial secondary metabolites, *Microb. Biotechnol.* 4(4), 471-8. [https://doi: 10.1111/j.1751-7915.2010.00196.x](https://doi.org/10.1111/j.1751-7915.2010.00196.x).
- Photos-Jones, E. , Keane, C., Jones, A.X., Stamatakis, M., Robertson, P., Hall, A.J., Leanord, A., 2015. Testing Dioscorides' medicinal clays for their antibacterial properties: the case of Samian Earth. *J. Arch. Sci.* 57, 257-267. (doi:10.1016/j.jas.2015.01.020)
- Photos-Jones, E. , Christidis, G.E., Piochi, M., Keane, C., Mormone, A., Balassone, G., Perdikatsis, V. and Leanord, A., 2016. Testing Greco-Roman medicinal minerals: The case of solfataric alum. *Journal of Archaeological Science: Reports*, 10, pp. 82-95. (doi:10.1016/j.jasrep.2016.08.042)
- Photos-Jones, E., Edwards, C., Häner, F., et al., 2017. Archaeological medicinal earths as antibacterial agents: the case of the Basel Lemnian sphragides. London, Geological Society, Special Publications 452. [https:// doi: 10.1144/SP452.6](https://doi.org/10.1144/SP452.6).
- Photos-Jones, E., Knapp, C.W., Venieri, D., Christidis, G.E., Elgy, C., Valsami-Jones, E., Gounaki, I., Andriopoulou, N.C., 2018. Greco-Roman mineral (litho)therapeutics

- 1012 and their relationship to their microbiome: The case of the red pigment *miltos*. J.
 1013 Arch. Sci. Rep. 22(12), 179-192. <https://doi.org/10.1016/j.jasrep.2018.07.017>.
- 1014 Photos-Jones, E., Hall, A.J., 2011. Lemnian Earth and the Earths of the Aegean: an
 1015 Archaeological Guide to Medicines, Pigments and Washing Powders. Glasgow,
 1016 Pottinger Press.
- 1017
 1018 Rao, M.P.N, Xiao, M., Li, W-J., 2017. Fungal and bacterial pigments: secondary
 1019 metabolites with wide applications. Front. Microbiol. 8, 1113.
- 1020
 1021 Samson, R.A., 2016. Cellular constitution, water and nutritional needs, and secondary
 1022 metabolites, in: ADD EDS : Environmental Mycology in Public Health. Elsevier.
 1023 <https://doi.org/10.1016/B978-0-012-411471-5.000001-6>.
- 1024
 1025 Saepua, S., Kornsakulkarn, J., Somyong, W., Laksanacharoen, P., Isaka, M., 2018.
 1026 Bioactive compounds from the scale insect fungus *Conoideocrella tenuis* BCC 44534.
 1027 Tetrahedron 74, 859-866.
- 1028
 1029 Swetha S, Santhosh S.M., Balakrishna R.G., 2010. Enhanced bactericidal activity of
 1030 modified titania in sunlight against pseudomonas aeruginosa, a water-borne
 1031 pathogen. Photochem Photobiol 86:1127–1134 . doi: 10.1111/j.1751-
 1032 1097.2010.00781.x
- 1033
 1034 Santos-Ebinuma, V.C., Teixeira, M.F.S., Pessoa Jr., A., 2013. Submerged culture
 1035 conditions for the production of alternative natural colorants by a new isolated
 1036 *Penicillium purpurogenum* DPUA 1275. J. Microbiol. Biotechnol. 23, 802-810.
- 1037
 1038 Sealy, F.L.W., 1919. Lemnos. Annual British School at Athens 22, 164–165.
- 1039 Tourptsoglou-Stephanidou, B., 1986. Ταξιδιωτικά και γεωγραφικά κείμενα για την
 1040 νήσο Λήμνο (15-20 αιώνας) (Geographic and Travellers' accounts for the island of
 1041 Lemnos (15th-20th century). University of Thessaloniki, Polytechnic School IX, Suppl
 1042 33.
- 1043
 1044 Tyc, O., Song, C., Dickschat, J.S., Vos, M., Garbeva, P., 2016. Ecological role of
 1045 volatile and soluble secondary metabolites produced by soil bacteria. Trends in
 1046 Microbiology 25(4), 280-92. <https://doi.org/10.1016/j.tim.2016.12.002>
- 1047
 1048 Wang, Q., Garrity, G.M., Tiedje, J.M. Cole, J.R., 2007. Naïve Bayesian Classifier for
 1049 Rapid Assignment of rRNA Sequences into the New Bacterial Taxonomy. Appl.
 1050 Environ. Microbiol. 73(16), 5261-5267. <https://doi.org/10.1128/AEM.00062-07>.
- 1051
 1052 Venieri D., Gounaki I., Bikouvaraki M., Binas V., Zachopoulos A., Kiriakidis G.,
 1053 Mantzavinos D., 2017a. Solar photocatalysis as disinfection technique:
 1054 Inactivation of *Klebsiella pneumoniae* in sewage and investigation of changes in
 1055 antibiotic resistance profile. J Environ Manage 195: . doi:
 1056 10.1016/j.jenvman.2016.06.009
- 1057
 1058 Venieri D., Tournas F., Gounaki I., Binas V., Zachopoulos A., Kiriakidis G.,
 Mantzavinos D., 2017b. Inactivation of *Staphylococcus aureus* in water by

1059 means of solar photocatalysis using metal doped TiO₂ semiconductors. J Chem
1060 Technol Biotechnol 92:43–51 . doi: 10.1002/jctb.5085
1061
1062
1063 Williams, L.B., 2017. Geomimicry: harnessing the antibacterial action of clays. Clay
1064 Miner. 52, 1-24.
1065
1066 Yilmaz, N., Visagie, C.M., Houbaken, J., Frisvad, J.C., Samson, R.A.,
1067 2014. Polyphasic taxonomy of genus *Talaromyces*. Stud. Mycology 78, 175-341.
1068
1069 Zarate-Reyes, L., Lopez-Pacheco, C., Nieto-Camacho, A., Palacios, E., Gómez-
1070 Vidales, V., Kaufhold, S., Ufer, C., García Zepeda, E., Cervini-Silva, J., 2018.
1071 Antibacterial clay against Gram-negative antibiotic resistant bacteria. J. Hazardous
1072 Materials 342, 625-632.
1073
1074